2D photocurrent and transmission mapping of aqueous dye sensitized solar cells.

Thomas A.G. Risbridger[1], Fernando A. Castro[2] and Petra J. Cameron[1]*

[1] 1 South, Department of Chemistry, University of Bath, BA2 7AY, United Kingdom.

[2] Materials Division, National Physical Laboratory, Hampton Road, Teddington, Middlesex, TW11 0LW, United Kingdom.

*Corresponding Author: p.j.cameron@bath.ac.uk

KEYWORDS Aqueous dye sensitized solar cells, dye sensitized solar cells, water, photocurrent mapping, transmission mapping, spatially resolved.

Abstract

There is currently renewed interest in aqueous dye sensitized solar cells (DSC). Water ingress in conventional DSC leads to a loss of efficiency, one solution to this problem is to optimize the cells to work in the presence of water. The aim is to create a stable cell and to avoid the need for buffer layers and encapsulation which increase device cost. Water containing electrolytes generally give lower photocurrents than those based on organic solvents, a problem that has in part been attributed to poor pore filling by the aqueous electrolyte. Here two sets of cells have been made which are identical except for the nature of the solvent (water or acetonitrile). Photocurrent mapping has been used to compare spatially resolved inhomogeneities in the current density. High-resolution transmission mapping (3906 data points/cm^2) has been used to decouple dye coverage and film thickness from electrolyte permeation. Filling cells using heating and vacuum was found to improve water electrolyte permeation. Photocurrent maps suggest that dye desorption occurs adjacent to the filling holes in both acetonitrile and water based cells; with significantly more dye desorbed in the water based cells. The loss of dye was attributed to desorption by the tert-butyl pyridine base in the electrolyte.

Introduction

Dye sensitized solar cells have seen ongoing improvements in recent years, with the current efficiency record standing at over 12%[1]. Many studies have looked at improving efficiency, but in order to be commercially viable, cells must also have good stability over a long period of time. The complex nature of the cell means that the stability of several components needs to be considered, along with their interaction with each other in the cells' working environment. The electrolyte has several important roles within the cell; most importantly it contains the redox mediator which acts to regenerate the oxidized dye after electron injection into the semi-conductor. The oxidized mediator then diffuses to the counter electrode where it is reduced. If the electrolyte deteriorates over time, there is a subsequent decrease in the cell performance, even to the point of cell failure. Two causes of degradation are the penetration of water into the cell[2], and the loss of volatile organic solvent to the environment via evaporation. Water ingress and organic solvent loss are particular problems in flexible cells on polymer substrates, or cells sealed with polymer[2-3]. In these cells it is almost impossible to prevent changes in the electrolyte composition over time. Water was used as the electrolyte solvent in the early days of DSC research[4], it was then abandoned as other solvents were found to give higher efficiencies. However, the use of water containing electrolytes has recently been reconsidered[5], and improvements in efficiency have been made. Law *et al.* have obtained efficiencies of up to 2.4% for 100% water cells containing the I^-/I_3^- redox couple, whereas Daeneke *et al* have obtained a 4% efficient aqueous ferricyanide cell[5b].

It appears that the major limiting factor for aqueous DSCs is the lower photocurrent density[5a], with the current decreasing as a function of the fraction of water content[6]. Law *et al.*[5a] saw both lower photocurrent densities at all illumination intensities and a clear limit in the measured

photocurrent at high (>0.55sun) light intensities. These observations were attributed to two causes. Firstly phase segregation in the I^-/I_3^- containing electrolyte within the semiconductor pores was thought to cause slow diffusion of the redox mediators leading to a diffusion limited photocurrent. The problem was observed for mixed water/methoxypropionitrile (MPN) systems containing the ionic liquid PMII. Secondly it was suggested that incomplete filling of the porous semi-conductor with electrolyte led to a reduction in the number of dye molecules that were being regenerated after electron injection. Water has a much higher surface energy than most organic solvents which can make pore filling more difficult. In addition, efficient water based DSC have only been produced using hydrophobic dyes to date[5] which exacerbate the problem of pore filling but are necessary to prevent large amounts of dye desorbing into the electrolyte. In our own work we have also obtained lower photocurrent densities for water containing DSC, but no limit with light intensity up to current densities of $10mAcm^{-2}$.[7]

One method that can give information on the relationship between electrolyte filling and photocurrent is spatially resolved photocurrent mapping. [2,8,9] Although information about pore filling cannot be obtained on the nanoscale, larger scale inhomogeneities can be observed. Photocurrent mapping has been used to examine the effect of damage and pressure on a cell[8], reasons for cell degradation[2] and dye stability[9]. A variation on this technique is that of visible transmission mapping, which can give information on the 2D dye coverage. Transmission mapping is not commonly used in DSC, although Barkschat *et al.* used a video camera in order to measure light transmission through a dyed film[9]. One practical difficulty in attributing changes in local current density to electrolyte filling is compensating for any dye inhomogeneity across the cell, or any effects on the dye caused by the addition of electrolyte. If the dye coverage can be

measured separately, then these effects can be examined, and a better picture of what is occurring in the cell obtained.

Here results from two related experiments are presented. Two sets of DSC's were made with different types of electrolyte – three containing water based electrolyte and three containing acetonitrile based electrolyte. In all other respects the DSC were identical. In the first set of experiments 2D photocurrent maps of these cells were measured. In the second set of experiments, three additional cells were examined at different stages in their production by both transmission mapping and photocurrent mapping.

Experimental

Full experimental details are given in the supporting information. In brief, the photocurrent of six DSCs made using either water or acetonitrile based electrolyte was measured as a function of 2D position using a laser mapping system with a wavelength of 532nm. Initial low resolution (625 data points/cm^2) measurements of six cells were made. A further three cells were then prepared and used for higher resolution (3906 points/cm^2) photocurrent and transmission measurements. All photocurrent maps were measured with bias illumination (white light, low intensity Halogen lamp). The transmission of the dyed film as a function of 2D position was recorded before these three cells were constructed. A photocurrent map was then measured for the completed cells, which were then taken apart to allow a final 2D transmission map of the photo anode to be measured. All the measurements were taken in plan view at ambient temperature.

Results and Discussion.

Measurements on two sets of cells are presented. The first set, AC1 – AC3 were made with MeCN based electrolyte and the second set, W1-W3 were made with water based electrolyte. All the cells were made using Z907 dye and an electrolyte optimized for water cells as described by Law *et al.*[10] Table 1 gives the cell characteristics before current mapping and table 2 gives the characteristics after current mapping. The average efficiency for the MeCN based cells was 2.4% and for the water based cells was slightly higher at 2.8% (1 Sun, AM1.5). The efficiencies obtained for the water based cells are very reasonable for 1cm^2 devices. Law[10] obtained an efficiency of 2.4% for similarly sized cells with the same electrolyte, although their cells showed photocurrent limitations at higher light intensities. Recently Daeneke *et al.*[11] obtained efficiencies of just over 4% for a 4mm^2 DSC containing the ferri/ferrocyanide couple. It is important to note that because the contents of the electrolyte were optimized for water, high efficiency acetonitrile cells are not expected. In our lab an optimized acetonitrile cell (N719, 1cm^2 area, no scattering layers, no $TiCl_4$ treatment) gives efficiencies just over 5% (1 Sun, AM 1.5). In our experiments the water cells did not show any limitations in photocurrent with light intensity (Figure 1.)

Cell	Solvent	I_{SC} / mA	V_{OC} / V	Fill Factor / %	η / %	Average η
AC1	MeCN/BuCN	6.4	0.665	64	2.9	
AC2	MeCN/BuCN	4.7	0.631	63	2.1	2.4±0.4
AC3	MeCN/BuCN	4.5	0.672	67	2.3	
W1	Water/Triton X-100	6.5	0.661	64	2.9	
W2	Water/Triton X-100	6.7	0.662	65	3.1	2.8±0.4
W3	Water/Triton X-100	4.6	0.692	67	2.4	

Table 1 Summary of cells characteristics before laser mapping measurements were taken.

Cell	Solvent	I_{SC} / mA	V_{OC} / V	Fill Factor / %	η / %	Average η
AC1	MeCN/BuCN	10.5	0.680	42	3.0	
AC2	MeCN/BuCN	5.6	0.659	52	1.9	2.4±0.5
AC3	MeCN/BuCN	4.9	0.695	64	2.2	
W1	Water/Triton X-100	6.9	0.704	59	2.9	
W2	Water/Triton X-100	6.8	0.704	63	3.0	2.8±0.3
W3	Water/Triton X-100	5.8	0.713	51	2.4	

Table 2 Summary of cells characteristics after laser mapping photocurrent measurement.

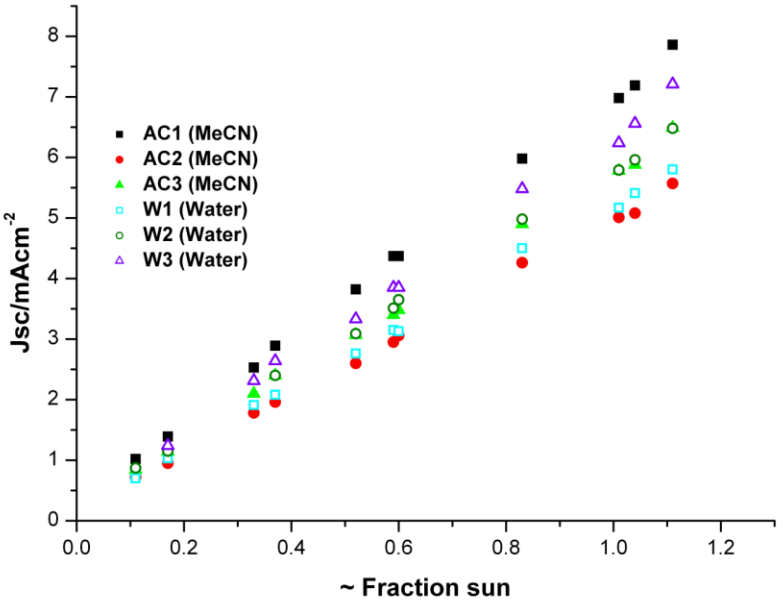

Figure 1. Photocurrent response from water and acetonitrile cells as a function of light intensity.

Low resolution photocurrent mapping and measurement repeatability.

Photocurrent mapping was carried out on all 6 cells, the step size was 400µm giving a resolution of 625 measurement points per square centimeter. The measurements were done using a white bias light across the whole cell area to ensure the cells were measured under steady state

conditions. In all cases the blue areas of zero photocurrent around the edges of the plots represent areas where no TiO_2 was present.

A number of repeats were measured initially on one cell containing an acetonitrile based electrolyte in order to determine the measurement repeatability (supporting information, Figures S1 and S2.). There was some deterioration of the cell photocurrent performance over multiple readings, particularly when measurements were taken immediately after one another. The performance recovered somewhat when the cells were stored in the dark for one hour but did not return to initial values within this period. IV curves taken before and after photocurrent mapping (tables 1 and 2) showed similar changes for both types of cells. After the measurements, photocurrent and voltage both increased while fill factor decreased resulting in essentially unchanged efficiencies. A detailed understanding of these effects is beyond the scope of this work but a possible explanation is suggested based on the work of Listorti *et al.*[12] who examined the effect of light soaking on dye cells. It is possible that the illumination incident on the cell from the bias and laser light led to a lowering in the conduction band (CB) of the semiconductor and subsequent increase in electron injection and photocurrent. Listorti *et al.* also saw a reduction in the recombination reaction between semiconductor electrons and I_3^-, negating the expected drop in photovoltage due to changes in CB position, and this may also partly explain the direction of the change in photovoltage observed here. The drop in fill factor could be explained by an increase in internal resistance. Macht *et al.* note that loss of iodine occurring in the electrolyte under illumination can lead to an increase of internal resistance and that this loss of iodine is favored at increased temperature[2]. The large changes in fill factor observed here may be due to localized heating effects from the 50 μm diameter laser spot. Interestingly, the cell used for degradation analysis (cell measured seven times, Figures S1 and S2 in the supporting

information) showed the largest increase in photocurrent, the smallest increase in photovoltage and the greatest decrease in fill factor of all the cells measured, which would be consistent with having a greater negative change to conduction band position compared to the other cells, and the largest increase in internal resistance, both of which could result from the increased exposure to light the cell received. The cells were not cooled during the measurements and the effect of temperature on cell performance is currently under investigation in a separate study.

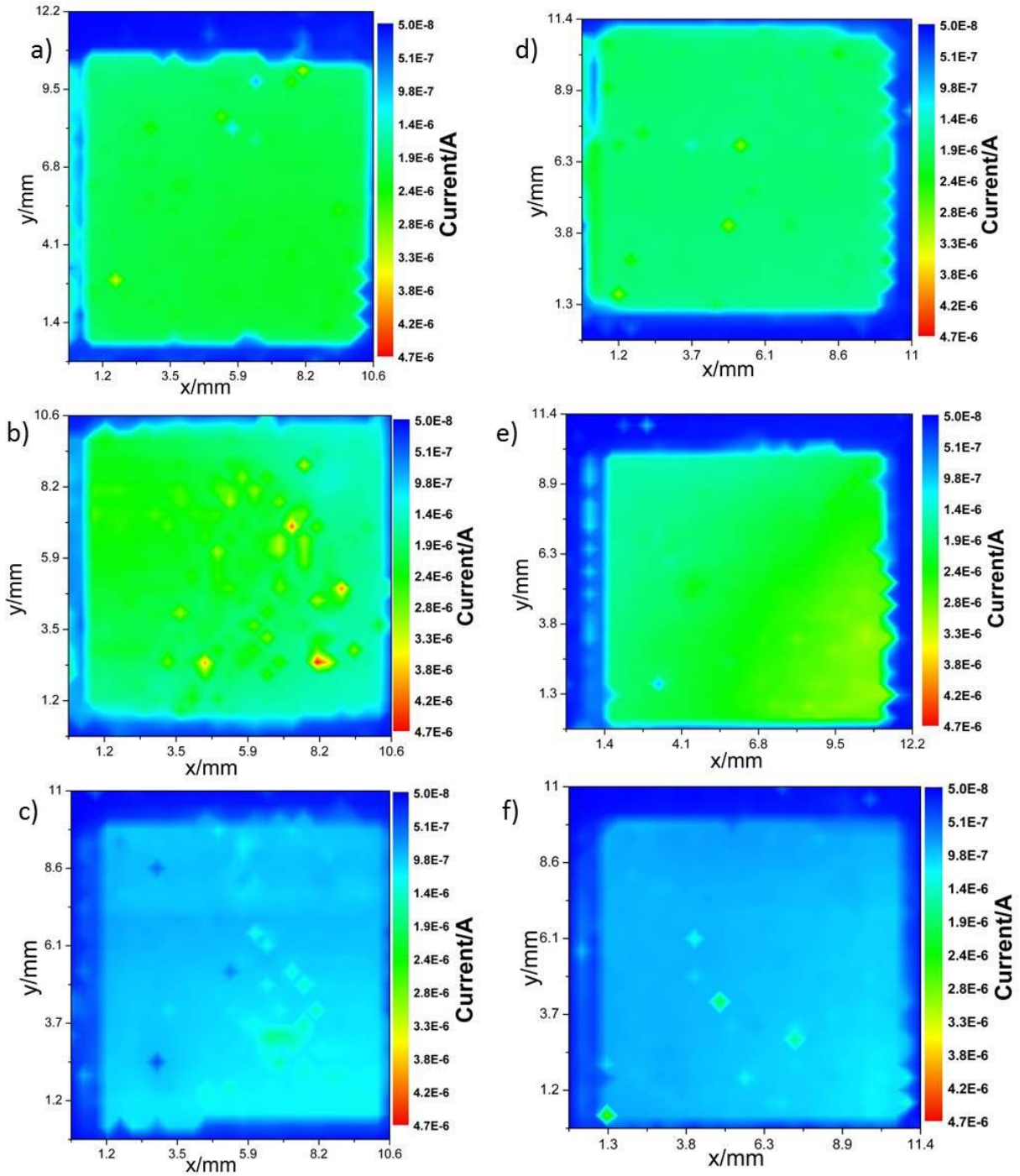

Figure 2. Photocurrent maps for three cells using acetonitrile based electrolyte a) AC1, b) AC2, c) AC3 and three cells using water based electrolyte d) W1, e) W2 and f) W3. Photocurrent is measured on the same intensity scale for each map in order to compare between cells. Filling holes are located in the bottom left and top right corners of each cell

Photocurrent maps of all six cells on the same intensity scale (relative to the maximum current) are shown in Figure 2. It can be seen that there are no obvious differences between the water and acetonitrile based cells. Figure 3 shows the same current maps scaled individually for each cell, making the inhomogeneities in the photocurrent maps clearer. Two of the acetonitrile cells, AC2 and AC3 showed slightly higher efficiencies in one corner. In the case of the water cells, W1 was quite homogeneous. W3 showed a slight increase in photocurrent in the bottom right hand corner. In contrast the photocurrent produced by W2 was very inhomogeneous.

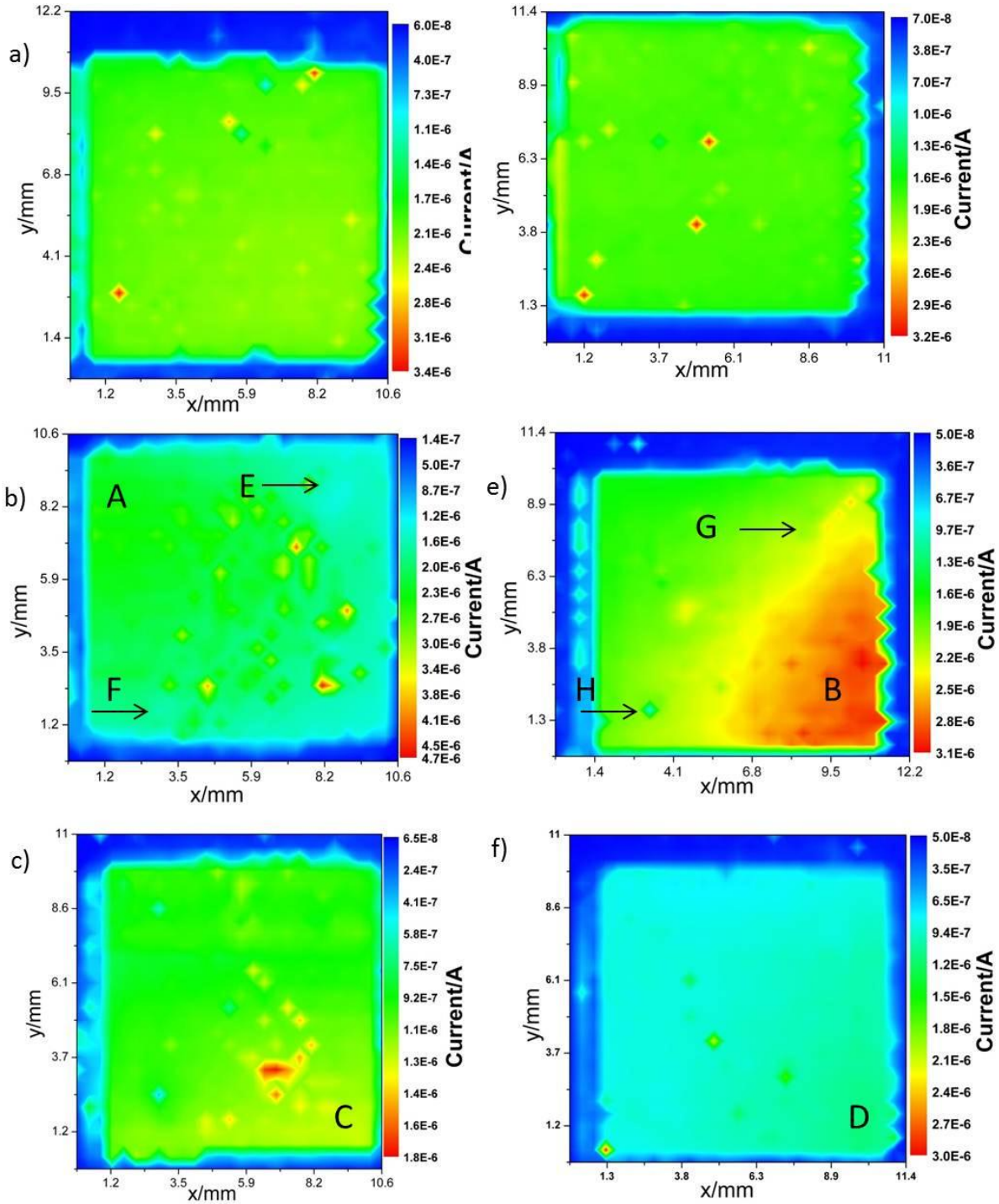

Figure 3. Photocurrent maps for three cells using acetonitrile based electrolyte a) AC1, b) AC2, c) AC3 and three cells using water based electrolyte d) W1, e) W2 and f) W3. Photocurrent is measured on a different scale for each map in order to emphasise features within each cell. Filling holes are located in the bottom left and top right corners of each cell and cold spots adjacent to the filling holes have been marked by black arrows where observed.

Miettunen *et al.*[13] saw a decrease in cell performance as they moved further from the electrolyte filling hole in their cells which they attributed to a decrease in local tert-butyl pyridine concentration as it was adsorbed strongly to the surface. A similar pattern is not observed in our measurements, with corners of high photocurrent sometimes corresponding to the filling holes and sometimes not (areas of higher photocurrent labeled A-D). In addition all cells were filled from two holes (two 0.6 mm diameter filling holes, a drop of electrolyte placed on each hole, filled under vacuum) and there was no clear pattern of higher photocurrent under both holes. This suggests that, in contrast to Miettunen, variation in current was not due to local adsorption of electrolyte species. Finally there was no evidence of poor pore filling in the water cells (heat and vacuum filled), which agrees with the lack of diffusion limitation seen on plots of photocurrent versus illumination intensity (Figure 1).

In several cells localized spots of lower photocurrent were seen directly under the filling holes (just visible in AC2 and W2, marked E,F,G and H) which will be discussed in more detail later. Transmission mapping suggests that, unsurprisingly, small differences in photocurrent could have been due to the local dye distribution in the film. Cells that leaked from the Surlyn gaskets showed large variations in photocurrent due to loss of electrolyte and a photocurrent map of a leaking cell is shown in the supporting information (Figure S3) for contrast.

It is more difficult to analyze the small spots of low/high photocurrent seen on many of the cells. Areas of reduced photocurrent may be due to dust particles or film imperfections. Small areas of high photocurrent may also be due to local differences in the TiO_2 films. The most important point is that no clear differences between the two sets of cells were observed. There was also no apparent relationship between homogeneity and efficiency.

Higher Resolution Photocurrent Mapping and Transmission Mapping.

Three cells were investigated in more detail using transmission mapping and high resolution photocurrent mapping. Transmission mapping was carried out on the photoanodes before they were assembled into cells (Figure 4), photocurrent maps were obtained (Figure 5) and finally transmission maps were measured again for the same anodes after the cells were disassembled (Figure 6). Transmission mapping was used to investigate whether variations in dye coverage or TiO_2 film thickness were responsible for the areas of high and low photocurrent in the DSC. High resolution photocurrent mapping was carried out using a step size of 160 μm giving 3906 data points/cm^2, and data was normalized with respect to the maximum transmission seen through the glass. Three cells were measured: AC4 containing an acetonitrile based electrolyte, W4 containing a water based electrolyte that was introduced under vacuum at room temperature and W5 containing a water based electrolyte introduced into the cell using both vacuum and heating.

It should be noted that in several of the cells, clear horizontal lines appeared (e.g. Figure 5(c)), separating areas of apparent variation in photocurrent. These lines are not seen in lower resolution scans (supporting information Figure S4) and appear then disappear between sequential high resolution readings; it is therefore likely that the lines are an artifact of the high resolution measurements. We excluded laser stability as a possible cause by measuring the laser output for prolonged times and confirming that no significant variations occurred. Therefore the lines are most likely due to small vertical positional changes between the laser and the sample caused by vibration. As the photocurrent changes appear as a step change in the measured values and are not reproduced between measurements it is easy to notice them and to remove them from the data interpretation.

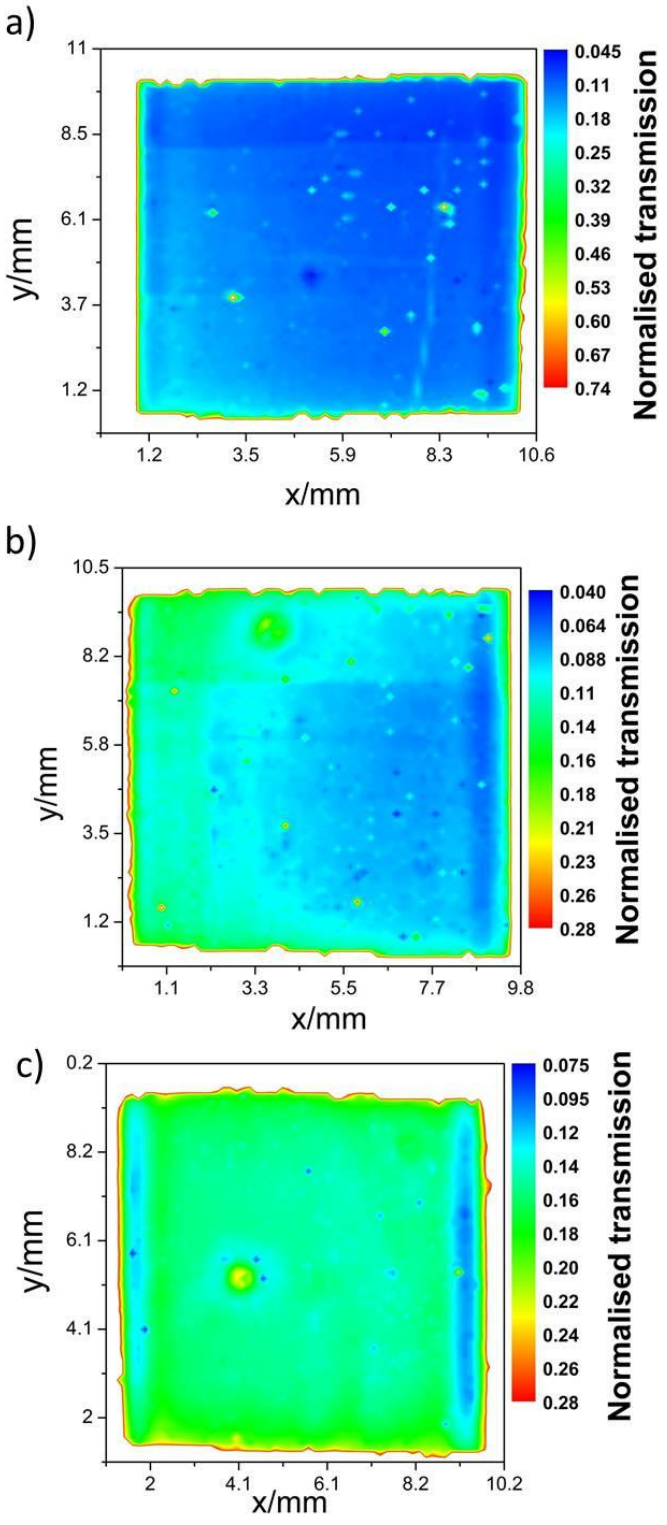

Figure 4. Transmission maps for dyed films before making into cells. Made into the following cells a) AC4 (acetonitrile), b) W4 (water) and c) W5 (water). Note that for transmission maps, blue represents lower transmission and so the greatest amount of dye.

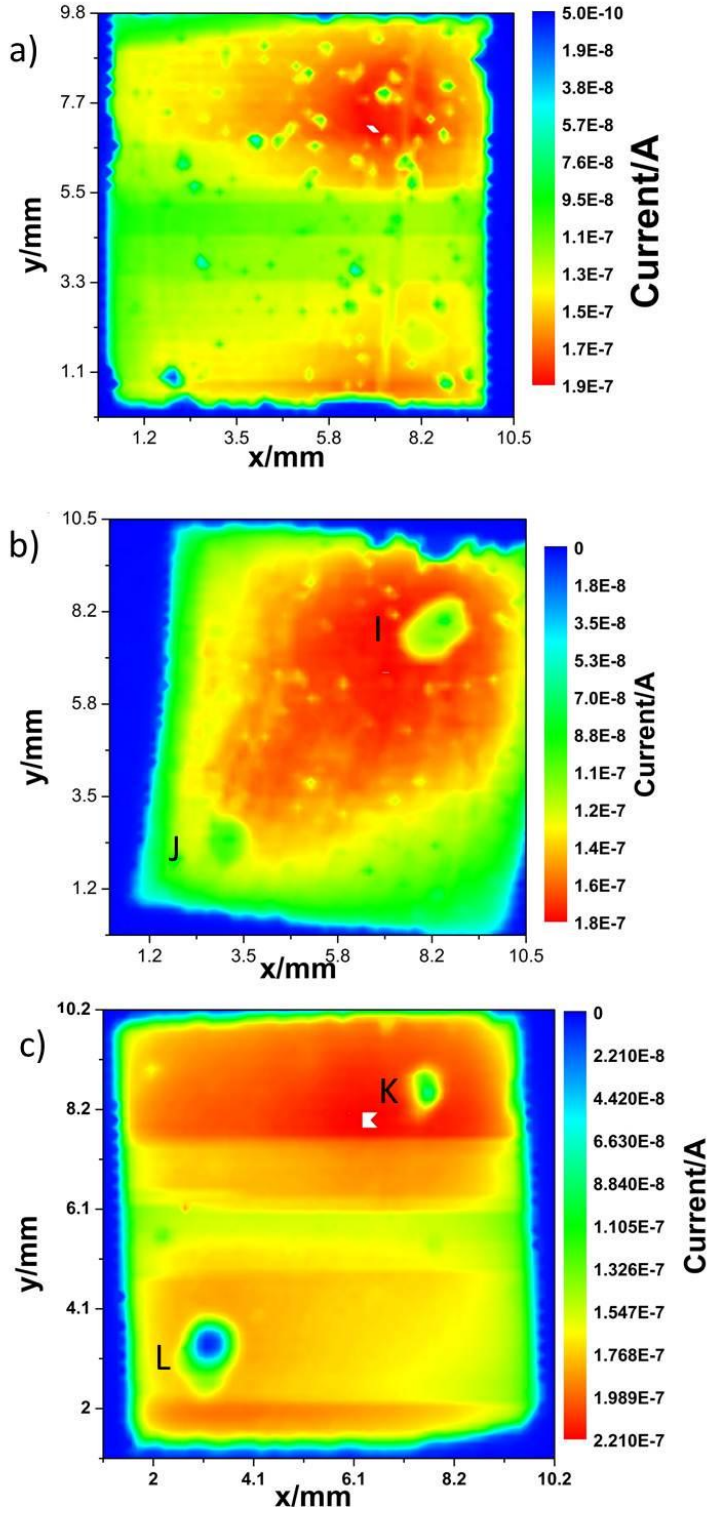

Figure 5. Photocurrent maps for cells a) AC4 (Acetonitrile, filled with only vacuum), b) W4 (Water, filled with only vacuum) and c) W5 (Water, filled with vacuum and heating). The positions of the filling holes and the corresponding cold spots are indicated by the letter I-L.

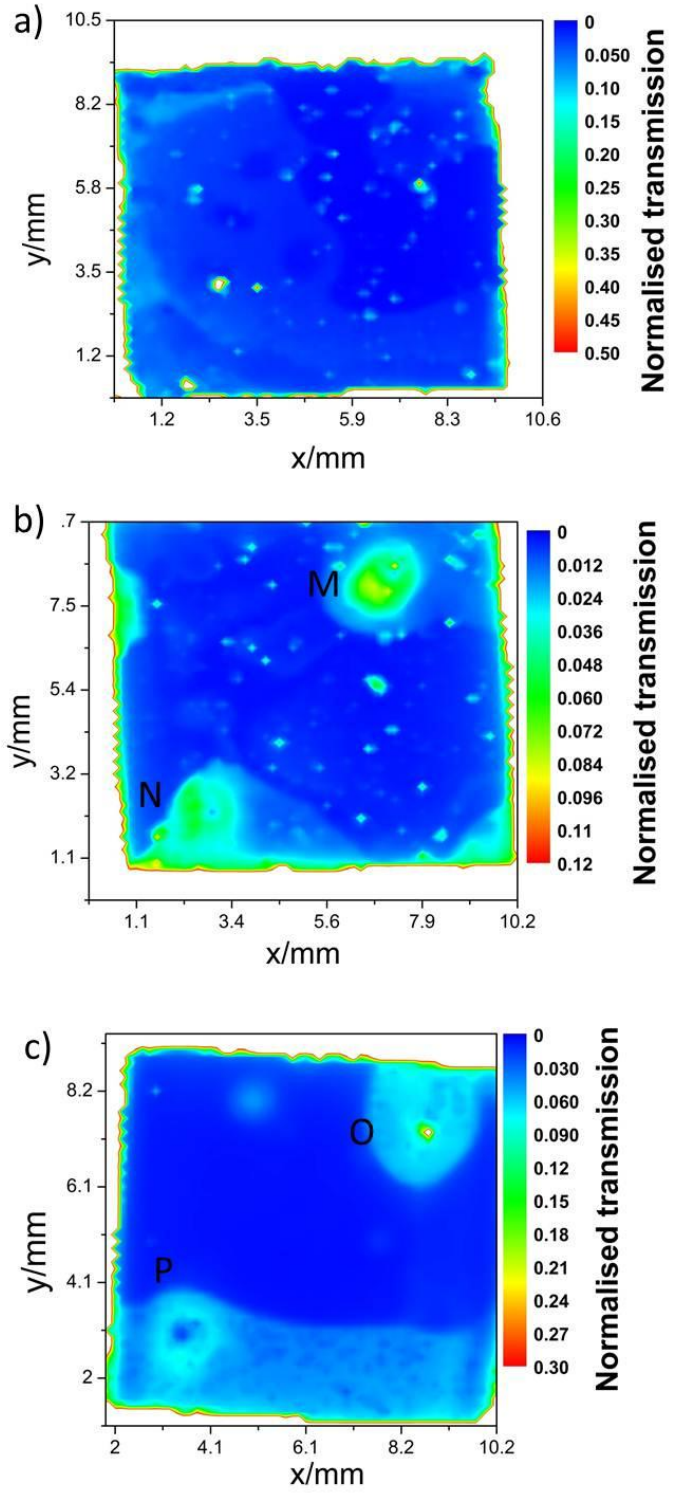

Figure 6. Transmission maps for dyed films after taking apart cells. Taken from the following cells a) AC4 (Acetonitrile, filled with only vacuum), b) W4 (Water, filled with only vacuum) and c) W5 (Water, filled with vacuum and heating)

AC4 (Acetonitrile cell, filled by vacuum no heating)

An area of high photocurrent was observed at the top of the cell (visible on the high resolution scan, figure 5(b), and on a low resolution scan, figure S4(a) supporting information). The area of enhanced photocurrent corresponds to an area of higher dye coverage as seen in the transmission map. This can be attributed to the TiO_2 film being slightly thicker on one side or an uneven dye uptake by the films which were placed vertically in the dye bath.

W4 (water cell, filled under vacuum but with no heat)

The photocurrent map (Figure 5(a)) shows an area of high photocurrent that spreads out from the filling hole (labeled I). Transmission mapping (Figures 4(a) and 6(a)) showed an area of lower transmission (higher dye concentration) on the right side of the film. The photocurrent map did not show any features that corresponded with the initial transmission mapping suggesting that the photocurrent map was dominated by the distribution of the electrolyte. This cell was filled at room temperature under vacuum, the photocurrent map suggests that pore filling was relatively poor under these conditions and may have limited the cell performance.

It is interesting to note that there are two clear areas of low photocurrent under the filling holes, it can further be seen from Figure 6(a) that the dye has been desorbed from the area of the photoanode under the holes.

W5 (water cell, vacuum filling with heating)

The current map for W5 (Figure 5(c)) suggests homogeneous current densities across the cell area. The horizontal lines showing areas of apparent differences in photocurrent are artifacts of

the measurement and disappear when lower resolution scans are taken (Figure S4(b)). The better homogeneity observed for this cell (and for cells W1-W3 above) was attributed to better electrolyte penetration due to pore filling at 80 ^{o}C under vacuum. Again two areas of low photocurrent were measured under the filling holes and corresponded to areas of low dye coverage in the final transmission maps (Figure 6(c) labeled K and L).

There are two possible explanations for the loss of photocurrent and dye seen adjacent to the filling holes in all three cells. Firstly there is no platinized counter electrode adjacent to this part of the anode and it is possible that there is some resulting degradation of the dye in these regions when the cell is under operation. The second explanation is that the flow of electrolyte passing over this region during cell filling causes some dye desorption.

The first explanation seems less likely for a number of reasons. Firstly the areas of desorbed dye are considerably larger in the water cells than in the acetonitrile cells, despite similar current densities under illumination. Finally in some of the water cells we observed the loss of dye by eye (Fig S5) even before the IV curve or the photocurrent map had been measured. Dye chemisorbs to the TiO_2 surface during dye sensitization, with the carboxylate-linked DSC dyes forming an ester bond with hydroxyl groups on the surface of the titania photo-anode; dye desorption can be achieved by treatment with alkali (usually NaOH) [14]. Recent studies have shown that other alkali solutions such as the tert-butyl pyridine commonly found in organic DSC electrolytes can also desorb dye from TiO_2 [15]. It is likely, therefore, that the 0.5 moldm^{-3} tert-butyl pyridine in the electrolyte is desorbing dye from the TiO_2 film under the filling holes creating areas of low photocurrent density. This dye desorption is significantly greater in water

based DSC than in acetonitrile based cells; although Figure 3(b) suggests that even in conventional DSC tert-butyl pyridine induced dye loss could be reducing cell efficiencies.

Conclusions

It can be concluded that the lower efficiency of water based DSC is at least partially due to dye instability with dye desorption occurring close to the filling holes. The development of efficient water stable dyes may be an effective way to increase the solar conversion efficiencies of water based DSC. There was some evidence that electrolyte filling also created cold spots in acetonitrile DSC, something which should be considered during the design and preparation of high efficiency DSC.

By measuring both photocurrent maps and transmission maps it has been possible to decouple dye and film thickness effects from variations caused by electrolyte across DSC surface. It has also been observed that an aqueous electrolyte filling method which involves heating the cell while under vacuum leads to improved electrolyte filling and better cell characteristics.

Finally the majority of DSC are characterized by reporting photocurrents and efficiencies that are an average from the whole cell area, the results reported here show that the non-homogeneity of cell photocurrents must be taken into account when optimizing cells.

Associated Content: Supporting information is available online

Acknowledgment: PJC thanks the EPSRC (EP/G031088/1) and the National Physical Laboratory for funding.

References

(1) Yella, A.; Lee, H. W.; Tsao, H. N.; Yi, C. Y.; Chandiran, A. K.; Nazeeruddin, M. K.; Diau, E. W. G.; Yeh, C. Y.; Zakeeruddin, S. M.; Gratzel, M. *Science* **2011**, *334*, 629-634.

(2) Macht, B.; Turrion, M.; Barkschat, A.; Salvador, P.; Ellmer, K.; Tributsch, H. *Sol. Energy Mater. Sol. Cells* **2002**, *73*, 163-173.

(3) Huang, L. T.; Lin, M. C.; Chang, M. L.; Wang, R. R.; Lin, H. C. *Thin Solid Films* **2009**, *517*, 4207-4210.

(4) (a) Matsumura, M.; Matsudaira, S.; Tsubomura, H.; Takata, M.; Yanagida, H. *Ind Eng Chem Prod Rd* **1980**, *19*, 415-421 (b) Matsumura, M.; Nomura, Y.; Tsubomura, H. *B Chem Soc Jpn* **1977**, *50*, 2533-2537 (c) Tsubomura, H.; Matsumura, M.; Nomura, Y.; Amamiya, T. *Nature (London)* **1976**, *261*, 402-403.

(5) (a) Law, C.; Pathirana, S. C.; Li, X.; Anderson, A. Y.; Barnes, P. R. F.; Listorti, A.; Ghaddar, T. H.; O'Regan, B. C. *Adv Mater* **2010**, *22*, 4505-4509 (b) Daeneke, T.; Uemura, Y.; Duffy, N. W.; Mozer, A. J.; Koumura, N.; Bach, U.; Spiccia, L. *Adv Mater* **2012**, *24*, 1222-1225.

(6) Liu, Y.; Hagfeldt, A.; Xiao, X. R.; Lindquist, S. E. *Sol Energ Mat Sol C* **1998**, *55*, 267-281.

(7) Risbridger, T., McCree-Grey, J., Cameron, P.J., Submitted, **2012**.

(8) Scott, M. J.; Woodhouse, M.; Parkinson, B. A.; Elliott, C. M. *J Electrochem Soc* **2008**, *155*, B290-B293.

(9) Barkschat, A.; Moehl, T.; Macht, B.; Tributsch, H. *Int J Photoenergy* **2008,** *2008,* 814951.

(10) Law, C. H.; Pathirana, S. C.; Li, X. O.; Anderson, A. Y.; Barnes, P. R. F.; Listorti, A.; Ghaddar, T. H.; O'Regan, B. C. *Adv Mater* **2010**, *22*, 4505-4509.

(11) Daeneke, T.; Uemura, Y.; Duffy, N. W.; Mozer, A. J.; Koumura, N.; Bach, U.; Spiccia, L. *Advanced Materials* **2012**, *24*, 1222-1225.

(12) Listorti, A.; Creager, C.; Sommeling, P.; Kroon, J.; Palomares, E.; Fornelli, A.; Breen, B.; Barnes, P. R. F.; Durrant, J. R.; Law, C.; O'Regan, B. *Energ Environ Sci* **2011**, *4*, 3494-3501.

(13) Miettunen, K.; Halme, J.; Lund, P. *Electrochem Commun* **2009**, *11*, 25-27.

(14) Holliman, P. J.; Vaca Velasco, B.; Butler, I.; Wijdekop, M.; Worsley, D. A. *International Journal of Photoenergy* **2008**, *2008*, 827605.

(15) P.J. Holliman, K. A.-S., M. Davies, A. Connell, UK Patent, submitted 26 January 2012.